The Effect of Amphotericin B on the Water and Nonelectrolyte Permeability of Thin Lipid Membranes

THOMAS E. ANDREOLI, VINCENT W. DENNIS, and ANN M. WEIGL

From the Department of Physiology and Pharmacology (Division of Clinical Physiology) and the Department of Medicine (Division of Nephrology), Duke University Medical Center, Durham, North Carolina 27706

ABSTRACT This paper reports the effects of amphotericin B, a polyene antibiotic, on the water and nonelectrolyte permeability of optically black, thin lipid membranes formed from sheep red blood cell lipids dissolved in decane. The permeability coefficients for the diffusion of water and nonelectrolytes (P_{D_i}) were estimated from unidirectional tracer fluxes when net water flow (J_w) was zero. Alternatively, an osmotic water permeability coefficient (P_f) was computed from J_w when the two aqueous phases contained unequal solute concentrations. In the absence of amphotericin B, when the membrane solutions contained equimolar amounts of cholesterol and phospholipid, P_f was 22.9 ± 4.6 μsec^{-1} and $P_{D_{H_2O}}$ was 10.8 ± 2.4 μsec^{-1}. Furthermore, P_{D_i} was < 0.05 μsec^{-1} for urea, glycerol, ribose, arabinose, glucose, and sucrose, and σ_i, the reflection coefficient of each of these solutes was one. When amphotericin B (10^{-6} M) was present in the aqueous phases and the membrane solutions contained equimolar amounts of cholesterol and phospholipid, $P_{D_{H_2O}}$ was 18.1 ± 2.4 μsec^{-1}; P_f was 549 ± 143 μsec^{-1} when glucose, sucrose, and raffinose were the aqueous solutes. Concomitantly, P_{D_i} varied inversely, and σ_i directly, with the effective hydrodynamic radii of the solutes tested. These polyene-dependent phenomena required the presence of cholesterol in the membrane solutions. These data were analyzed in terms of restricted diffusion and filtration through uniform right circular cylinders, and were compatible with the hypothesis that the interactions of amphotericin B with membrane-bound cholesterol result in the formation of pores whose equivalent radii are in the range 7 to 10.5 A.

INTRODUCTION

The characterized polyene antibiotics comprise a group of cyclic, amphipathic lactones, which contain a number (usually 4–7) of conjugated —C=C— double bonds in the ring structure, and have molecular weights in the range 500 to 1300 (1). With few exceptions, the biologic effects of these

drugs have been attributed to the increased cellular permeability to a variety of solutes which results from the interaction of the polyene compounds with membrane-bound sterols (2, 3). However, the detailed nature of such interactions is not clear.

Previous reports from this laboratory (4, 5) indicated that certain polyene antibiotics (nystatin and amphotericin B, but not filipin) strikingly reduced the DC resistance (R_m) of thin lipid membranes separating two aqueous phases, but only when the mole fraction of cholesterol in the lipid solutions used to form membranes exceeded 0.2 (5). Under these conditions, the reduction in DC membrane resistance was proportional to a high power (approximately 4.5) of the nystatin concentration in the aqueous phases. Consequently, it seemed likely that the primary unit responsible for the increases in the conductance of individual ions comprised a multimolecular aggregate of polyene antibiotic with membrane-bound cholesterol (4, 5). Furthermore, if such multimolecular units participated directly, rather than cooperatively, in the reduction in DC membrane resistance, it was inferred that they might form fixed sites, or pores, within the membrane phase (5). In order to gain additional information concerning this question, we have evaluated the effects of amphotericin B on the permeability of thin lipid membranes to water and nonelectrolytes. The experimental data provide support for the hypothesis that, in these membranes, the interaction of amphotericin B with membrane-bound cholesterol results in the formation of aqueous channels, or pores. Furthermore, if the pores are treated operationally as uniform right circular cylinders (6), in which the frictional interactions (7) between water and solutes are the same as in bulk solution, their effective radii can be estimated to be in the range of 7 to 10.5 A.

A preliminary report of the osmotic studies reported in this paper has appeared elsewhere (8).

METHODS

Lipids were extracted from high potassium (HK) sheep red blood cells (9), and depleted of cholesterol by acetone treatment (5). Unless otherwise indicated, the lipid solutions used to form membranes (membrane solutions) contained equimolar amount of cholesterol (Calbiochem, Los Angeles, Calif.) and HK sheep red blood cell lipids (92% phospholipid [5]) dissolved in decane at a concentration of 35–45 mg total lipid per ml decane (5, 9). The membrane solutions were applied with a brush technique (10) to an aperture (see below) separating two aqueous phases. As in previous studies (5, 9), all experiments were carried out at room temperature (22–24°C), and the aqueous phases were unbuffered (pH $\sim$ 5.8). Amphotericin B (batch No. 91368-001) was kindly furnished by Miss Barbara Stearns, Squibb Institute for Medical Research, New Brunswick, New Jersey. On the day of an experiment, a stock solution of the antibiotic dissolved in methanol ($1–2 \times 10^{-4}$ M) was prepared and stored at 4°C, and diluted in the aqueous phases immediately prior to use (5). Thus, the aque-

ous amphotericin B solutions contained 0.5–1.0% methanol. In control experiments, aqueous solutions containing 1.5% methanol did not modify the water, electrolyte, or nonelectrolyte permeability properties of the membranes. Tritiated water (THO) and ^{14}C-tagged nonelectrolytes (purity > 98.5%) were obtained from New England Nuclear Corp. (Boston, Mass.). The electrical and analytical determinations, techniques, and reagents were the same as in previous studies (5, 9), except for the modifications to be described below.

Unidirectional Tracer Fluxes

A schematic representation of the "isotope chamber" apparatus used in the unidirectional tracer flux experiments is shown in Fig. 1. The aqueous chambers (Fig. 1, front and rear) were symmetrical, open, square Lucite cells, 1.27 cm on a side and 1.2 cm deep, with input apertures (Fig. 1, *i*) for electrodes and fluid infusion. One

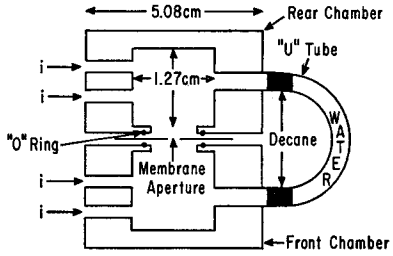

FIGURE 1. Schematic top view of isotope chamber apparatus. Details are in the text (Methods).

face of each chamber was open and guarded by a rubber "O" ring. The partitions containing the apertures (1.5 mm diameter) on which the membranes were formed were inserted between the two O rings and the entire apparatus was bolted together (the bolts are not pictured in Fig. 1). Two types of partitions were employed: stainless steel, either 0.125 mm (11) or 0.025 mm thick, and polyethylene, 0.125 mm thick. An area of the partitions surrounding the membrane aperture was abraded slightly and the partitions were washed initially with detergent and 50% ethanol and rinsed exhaustively with deionized water (9). Subsequently, the partitions were passed through acetone and stored under petroleum ether. Prior to use, the partitions were air-dried for approximately 1 hr.

Perfusion of one or both chambers, simultaneously or independently, at rates of 2–10 ml/min, was carried out by infusing fluid with a peristaltic pump into the input apertures, and aspirating through constant vacuum needles set at exactly the same height (0.3–0.6 cm) from the top of each chamber. Thus, the vacuum needles maintained nearly constant and identical upper limits to the volumes of fluid in the two chambers. Small magnetic stirring bars were placed at the floor of each chamber, and both aqueous phases were stirred vigorously (11) during the course of all isotope exchange experiments. It should be noted that the stirring rates could not be rigorously regulated, but were adjusted to provide maximal stirring (approximately 50–60 rpm) and visible oscillation of the membranes without rupturing the latter. To minimize heating of the aqueous phases from the magnetic stirrer, the chambers were set on rubber mounts 1.0 cm above the stirrer.

In order to maintain equal hydrostatic pressures in the two aqueous phases, both chambers were connected with a horizontal "U" tube (Tygon tubing, approximately 0.48 cm I.D.). A portion of the tube (a length of approximately 0.5 cm near the entrance to each chamber) was filled with decane, and the remainder was filled with water. This arrangement insured mechanical stability of the membranes despite considerable manipulation (i.e., perfusion or sampling) of the solutions in either chamber. In practice, shifts of the decane columns during frequent, intermittent perfusion and sampling of both chambers resulted in less than a 5% change in the aqueous volumes of the chambers during, for example, a typical 2 hr experiment.

Whenever isotopes were added to one aqueous phase, both chambers were covered with Parafilm lids to minimize contamination of the "cold" chamber by evaporation (12) or surface adsorption. To test for the absence of electrical or isotopic shunt pathways between the two chambers, an unperforated polyethylene partition was clamped between the two chambers. Under these conditions, the DC resistance between the two aqueous phases was $> 10^{12}$ ohms, and, when one aqueous phase contained approximately 5×10^6 counts min^{-1} ml^{-1} of either THO or ^{14}C-urea, no radioactivity above background levels was detected in fluid samples from the other aqueous phase, even after 12 hr periods. In addition, the electrical properties of membranes formed in this apparatus were the same as those observed when the front and rear chambers were isolated from one another (5, 9).

The unidirectional tracer flux experiments were carried out in the following manner. Thin lipid membranes were formed in the "isotope" chamber. The aqueous phases contained identical, dilute solutions (0.01 M; for THO flux experiments, the solute was urea or sucrose; for the flux of ^{14}C-nonelectrolytes, the solute corresponded to the isotope). 30 min after formation of a membrane, 0.1–0.15 ml background samples were taken from both chambers (using micropipettes), the aqueous volumes were readjusted, and THO or ^{14}C-tagged nonelectrolyte (final concentration ≈ 1–9×10^6 counts min^{-1} ml^{-1}) was added to the rear chamber. After approximately 5 min, a 20 μl sample was taken from the rear chamber. At the end of a flux period (15–20 min), a 0.1–0.15 ml sample was withdrawn from the front chamber. Subsequently, the front chamber was flushed completely (5 min; 8 ml/min) and the volumes of both chambers were readjusted. The flux periods were then repeated for the duration of the membrane, before and after the addition of amphotericin B to both aqueous phases. In practice, on any given day, at least one control flux period was carried out before the addition of amphotericin B to the aqueous phases. This procedure minimized the possibility that, for a given experiment, the observed effects were due to "shunt" pathways in the apparatus. The samples were adjusted to a uniform volume (0.1–0.15 ml), placed in 10 ml of Bray's phosphor (13), and counted for 10 min in a Tricarb (Packard Instrument Co., Downers Grove, Ill.) liquid scintillation counter. For a 10 min period, the average background counting rate was 400 ± 60 counts. Sufficient isotope was added to the rear chamber so that a counting rate of at least 400–500 counts above background per 10 min in a front chamber sample would correspond to a solute or water diffusion permeability coefficient (see below) of approximately 0.09–0.1×10^{-4} cm sec^{-1}. Accordingly, we could expect to detect reproducibly a minimum solute or water diffusion permeability coefficient of approximately 0.05×10^{-4} cm sec^{-1}. Consequently, when the counts in the front chamber

were not significantly greater than background, the results were reported as diffusion permeability coefficients $<0.05 \times 10^{-4}$ cm sec^{-1} (Table II), although the actual values may have been considerably lower.

A representative experiment illustrating the properties of the system is shown in Fig. 2. It should be noted that the rates of isotope exchange (Fig. 2, open symbols) were independent, within experimental error, of the duration of the membrane, and that the isotope concentration in the front chamber at the end of the flux period was negligible ($<1\%$) with respect to the isotope concentration in the rear chamber. Furthermore, the absence of significant counting rates greater than background in samples taken from the front chamber after the latter was flushed (Fig. 2, closed symbols) indicates the effectiveness of the rinsing procedure.

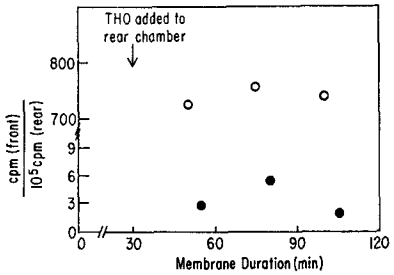

FIGURE 2. A representative tracer flux experiment. Ordinate, total counts min^{-1} (cpm) above background (front chamber) per 10^5 cpm (rear chamber); abscissa, membrane duration. The membranes were formed in 0.01 M urea; at 30 min, THO ($\sim 4 \times 10^6$ cpm/ml) was added to the rear chamber. Samples were taken from the front chamber before (open symbols) and after (closed symbols) flushing the front chamber for 5 min (8 ml/min). Experimental details are in Methods.

In these experiments, the two aqueous phases bathing the membranes contained the same volumes of dilute solutions, which were identical except for the concentration of isotope. Furthermore, the volumes of both aqueous phases were nearly constant (see above), the isotope concentration in the front (cold) chamber was zero at zero time (i.e., the start of any flux period), and negligible, during any flux period, with respect to the isotope concentration in the rear (hot) chamber (Fig. 2), which was very nearly constant. Accordingly, J^*_i, the unidirectional flux of the ith isotope across membranes per unit time during a given flux period, is:

$$J^*_i = \frac{C^*_{if}}{\Delta t} V_f \tag{1}$$

where C^*_{if} = concentration of isotope (counts min^{-1} ml^{-1}) in the front chamber aqueous phase, Δt = duration of the flux period, and V_f = volume of front chamber aqueous phase. In addition, under these conditions, $\vec{J}_i$, the unidirectional flux of water or of the ith solute across the membranes per unit time, is:

$$\vec{J}_i = \frac{J^*_i}{X_r} \tag{2}$$

where X_r = specific activity of the ith isotope (counts min^{-1} $mole^{-1}$) in the rear chamber aqueous phase. In view of the experimental conditions:

$$J_w = 0; J_w \approx J_v \tag{3}$$

where J_w and J_v = net water or volume flow, respectively, per unit area of membrane per unit time. As a consequence, it is a reasonable assumption that, in this situation, the unidirectional flux of water or of the ith solute may be described by Fick's first law. Thus, if the membrane is homogeneous, the aqueous phases are uniform, and the two membrane surfaces are in equilibrium with their adjacent aqueous phases:

$$\vec{J}_i = -\frac{D_i}{\Delta x} A_m C_r \tag{4}$$

where D_i = apparent, or restricted (14, 15) diffusion coefficient of water or of the ith solute, A_m = membrane area (measured experimentally by a calibrated reticle in the eyepiece of a low-power stereomicroscope), Δx = membrane thickness, C_r = concentration of water or the ith solute in the rear chamber aqueous phase, and,

$$P_{D_i} \equiv \frac{D_i}{\Delta x} \tag{5}$$

where P_{D_i} = permeability coefficient (cm sec^{-1}) for diffusion of water or the ith solute. Kedem and Katchalsky's ω_i, the solute permeability coefficient when $J_v = 0$ (16) is, to a sufficient approximation (17):

$$\omega_i = \frac{P_{D_i}}{RT} \tag{6}$$

where R = gas constant and T = absolute temperature. Alternatively, assuming restricted diffusion of water or of the ith solute through a number of sites in the membrane:

$$P'_{D_i} = \frac{P_{D_i}}{D_i^o} = \frac{A_{p_i} A^{-1}_m}{\Delta x} = \frac{A_{d_i}}{\Delta x} \tag{7}$$

where D_i^o = free diffusion coefficient of water or of the ith solute, A_{p_i} = the restricted area of the membrane available for diffusion of water or of the ith solute, A_{d_i} = the restricted area per 1 cm^2 membrane area for diffusion of water or of the ith solute, and P'_{D_i} (cm^{-1}) = restricted area per unit membrane thickness available for diffusion of water or the ith solute in a 1 cm^2 membrane.

Osmotic Flux Experiments

The experimental apparatus used in the osmotic flux experiments was similar to those described previously by other workers (11, 18, 19), and is illustrated schematically in Fig. 3. The rear chamber was formed from joined lengths of polyethylene tubing (11). One end of the tubing (1.8 mm I.D.) was sealed into a single front isotope chamber

and constituted the membrane aperture; the narrow end (0.29 mm I.D.) of the tubing was attached to a 10 μl syringe (No. 701N; Hamilton Co., Whittier, Calif.), and the shaft of the syringe was attached to a micrometer (18, 19). Both chambers were filled with the same aqueous phase (solute concentration = 0.01 molal), and the membranes were formed on the membrane aperture. 30 min after membrane formation, solutions containing higher solute concentrations were introduced into the front chamber, and the net water flux was estimated by measuring the micrometer displacement (i.e., the volume of fluid injected into the rear chamber) required to maintain an optically planar membrane (11, 18, 19). In these experiments, the total micrometer scale was 1000 units, and one micrometer unit corresponded to 4.8×10^{-6} ml. In practice, micrometer readings were taken every 1–2 min for a 15–30 min period, and the volume flow of water was estimated from the slope of the line relating micrometer displacement to time. Subsequently, the original, dilute solution was flushed into the front

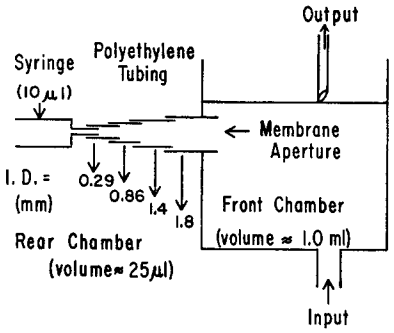

FIGURE 3. Schematic illustration of "osmotic" chamber apparatus. Details are in the text (Methods).

chamber and the flux periods were repeated for the duration of the membrane. For a given osmotic gradient, these slopes were independent, within the limits of experimental error, of the duration of the membrane.

Under these experimental conditions, mechanical hydrostatic pressure differences were negligible with respect to osmotic pressure differences. Accordingly, J_w, the net volume flow of water per unit area of membrane per unit time, is given by (16):

$$J_w = -\sigma_i L_p \Delta\pi, \qquad (8)$$

where σ_i = reflection coefficient of the ith solute (20), L_p = coefficient of hydraulic conductivity (16, 21), and $\Delta\pi$, the difference in osmotic pressure in the two aqueous phases bathing the membrane is:

$$\Delta\pi = RT(g_{r_i}c_{r_i} - g_{f_i}c_{f_i}) \qquad (9)$$

where c_{r_i} and c_{f_i} = osmolal solute concentration of the ith solute in the rear and front chambers respectively, and g_{r_i} and g_{f_i} their respective osmotic coefficients. As illustrated in Fig. 4, J_w was linear, within experimental error, with respect to $\Delta\pi$, in the range 2.5 to 20 atm. For any given experimental condition, $J_w/\Delta\pi$ was estimated from a minimum of two solute concentration differences in the two aqueous phases bathing the membranes. For comparison with the tracer flux experiments, the re-

sults were expressed in terms of an osmotic permeability coefficient, P_f (cm sec^{-1}), given by:

$$P_f = \sigma_i L_p \frac{RT}{\bar{V}_w} \tag{10}$$

where $\bar{V}_w$ = partial molar volume of water. Thus, when σ_i for a given solute was one (σ_i was assumed to be one when P_f was independent of the effective hydrodynamic radius of the aqueous solute), L_p could be computed from Equation 10, and, concomitantly, σ_i for more permeable solutes.

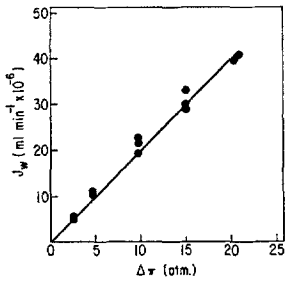

FIGURE 4. Net water flow (ordinate) as a function of the difference in osmotic pressure ($\Delta\pi$) in the two aqueous phases bathing the membrane. The membranes were formed in 0.01 molal sucrose; solutions of increasing sucrose concentration were introduced into the front chamber, and J_w was estimated as described in the text. A total of five membranes from one lipid preparation was used. Experimental details are in Methods.

RESULTS

The Permeability Coefficient for Diffusion of Water

The results of the tracer flux studies with THO are summarized in Table I. Under "standard" conditions (i.e., partition thickness = 1.25×10^{-2} cm, vigorous stirring in the aqueous phases, and equimolar amounts of cholesterol and phospholipid in the membrane solution), the value of P_{D_w} was $10.8 \pm 2.4 \times 10^{-4}$ cm sec^{-1}. This corresponds closely to the P_{D_w} value observed by Cass and Finkelstein (11) under quite similar experimental conditions (in particular, with a partition thickness = 1.25×10^{-2} cm and equimolar amounts of cholesterol and phospholipid in the membrane solutions) and is two to four times greater than the values originally reported by Huang and Thompson (18) or Hanai and Haydon (19), who did not utilize stirring in the aqueous phases. More recently Everitt, Redwood, and Haydon (22), employing thermal convection and/or mechanical stirring to produce mixing in the aqueous phases, have obtained P_{D_w} values for lecithin-cholesterol-decane membranes in the range 8.2 to 12.3×10^{-4} cm sec^{-1}. Cass and Finkelstein (11) have shown that P_{D_w} is reduced when the thickness of the partition on which the membranes are formed is $\geqq 2 \times 10^{-1}$ cm, presumably because,

at such thicknesses, mixing of boundary layers (24–26) in the aqueous phases adjacent to the membranes is diminished. However, as indicated in Table I, the values of P_{D_w} and, by inference, of any unstirred aqueous regions adjacent to the membranes, were independent of partition thickness (in the range of 0.25 to 1.25 $\times$ 10^{-2} cm).

TABLE I

THE PERMEABILITY COEFFICIENT FOR DIFFUSION OF WATER (P_{D_w}) IN THIN LIPID MEMBRANES

Membranes	Partition thickness	Membrane solution		P_{D_w}	A_{d_i}
		Cholesterol (M) / Phospholipid (M)	Amphotericin B		
(No.)	($cm \times 10^2$)		M	$cm\ sec^{-1} \times 10^4$	$\times 10^5$
7	1.25	1.0	0	10.8±2.4(10)	2.8
3	0.25	1.0	0	10.1±1.0(6)	2.62
11	1.25	1.0	10^{-6}	18.1±2.4(16)	4.68
10	1.25	0.05	0	14.0±4.1(18)	3.63
3	1.25	0.05	10^{-6}	11.9±1.3(6)	3.08

Thin lipid membranes were formed in the isotope chambers. The aqueous phases contained 0.01 M urea or 0.01 M sucrose and the indicated concentrations of amphotericin B. The thickness of the partitions and the composition of the membrane solutions are listed in the table. P_{D_w} was computed from Equation (4) and is expressed as the mean ± standard deviation (SD) for the indicated number of membranes. The numbers in parentheses indicate the number of observations (i.e., flux periods). A_{d_i}, the restricted area per 1 cm^2 membrane area for the diffusion of water was computed from Equation (7) and the mean values of P_{D_w}, assuming Δx, the membrane thickness, to be 60 A (12), and $D^0_w = 2.36 \times 10^{-5}$ cm^2 sec^{-1} (23).

The Effect of Amphotericin B on P_{D_w}

As indicated previously, amphotericin B strikingly reduces the DC resistance of these thin lipid membranes, and concomitantly renders them anion-selective, if the membranes are formed from lipid solutions containing a substantial fraction of cholesterol (5). Similarly, as illustrated in Table I, the drug increased by ~70% the values of P_{D_w} when the membranes were formed from lipid solutions containing equimolar amounts of cholesterol and phospholipid. P_{D_w} was also increased approximately 30% by reducing the molar ratio of cholesterol to phospholipid in the membrane solutions to <0.05 (see below). In this instance, the presence of amphotericin B (10^{-6} M) in the aqueous phases did not increase P_{D_w}. Although the values of P_{D_w} in the presence of amphotericin B (when the molar ratio of cholesterol to phospholipid in the membrane solutions was 1.0) and in the absence of the antibiotic (when the molar ratio of cholesterol to phospholipid in the membrane

solutions was <0.05) reflect differences of small statistical significance, the data are consistent with the cholesterol requirement for the amphotericin B–dependent increases in $P_{D_{urea}}$ (Table III) and P_f (Table V).

TABLE II

THE PERMEABILITY COEFFICIENT FOR DIFFUSION OF NONELECTROLYTES IN THIN LIPID MEMBRANES

Solute	r_i	B_i	Amphotericin B (M) M) = 0		Amphotericin B (M) = 10^{-6}		ω_i
			Membranes	P_{D_i}	Membranes	P_{D_i}	
	A	$\times 10^3$	(No.)	cm $sec^{-1} \times 10^4$	(No.)	cm $sec^{-1} \times 10^4$	$\frac{mole}{cm\ sec\ atm.} \times 10^9$
Urea	1.8	0.15	4	<0.05 (6)	4	10.4±0.9 (10/10)	41.6
Acetamide	2.5	0.83	3	0.83±0.17 (6)	4	5.48±1.42 (9/9)	21.9
Glycerol	3.1	0.07	2	<0.05 (4)	5	3.28±1.12 (11/11)	13.1
Ribose	3.6	—	—	—	5	0.61±0.16 (9/9)	2.44
Arabinose	3.8	—	2	<0.05 (4)	4	0.53±0.15 (10/10)	2.12
Glucose	4.2	—	3	<0.05 (5)	8	0.14±0.02 (8/16)	0.56
Sucrose	5.2	0.03	3	<0.05 (6)	13	~0.09 (4/22)	<0.5

Thin lipid membranes were formed in the isotope chambers. The aqueous phases contained the indicated solute (0.01 M), and the corresponding ^{14}C-tagged isotope (1–9 $\times 10^6$ cpm/ml) was added to the rear aqueous phase. Amphotericin B, when present, was in both aqueous phases. The partition thickness was 1.25×10^{-2} cm, and the membrane solutions contained equimolar amounts of cholesterol and phospholipid. The effective hydrodynamic radius, r_i, of each of the solutes except acetamide was obtained from Schultz and Solomon (27), and that of acetamide from Soll (28). The olive oil–water partition coefficients, B_i, of the solutes were obtained from Collander and Barlund (29). P_{D_i} was computed from Equation (4) and is expressed as the mean ± SD for the indicated number of membranes. As discussed in the text, the P_{D_i} values listed as <0.05 represent maxima, and the actual values may have been substantially lower. The single numbers in parentheses (in the absence of amphotericin B) indicate the number of flux periods. When amphotericin B was present the denominator in parentheses indicates the number of flux periods, and the numerator, the number of periods in which significant radioactivity was detected in the front chamber samples, from which the values of P_{D_i} were computed. The values of ω_i (16, 17) were computed from the mean P_{D_i} values and Equation 6.

The Permeability Coefficient for Diffusion of Nonelectrolytes

Table II lists the apparent diffusion permeability coefficients (P_{D_i} and ω_i) of certain nonelectrolytes for these thin lipid membranes. When amphotericin B was not present, P_{D_i}, for each of the solutes tested, except acetamide, was less than the minimum value (approximately 0.05×10^{-4} cm sec^{-1}) which could be detected under the present experimental circumstances, and negligible with respect to P_{D_w}. These data are in accord with the studies of Vreeman (30), who observed P_{D_i} values of 0.042×10^{-4} cm sec^{-1}, 0.045×10^{-4} cm sec^{-1}, and 0.007×10^{-4} cm sec^{-1}, for, respectively, urea, glycerol, and erythritol, in lecithin-cyclohexane–carbon tetrachloride membranes.

Thus it is likely that the actual values of P_{D_i} (particularly for ribose, glucose, and sucrose) were substantially less than 0.05×10^{-4} cm sec^{-1}. In contrast, $P_{D_{acetamide}}$ in the native membranes was at least 10 times greater than P_{D_i} for the other solutes tested (Table II). In this regard, it is of interest to note that the effective hydrodynamic radius of acetamide is intermediate between that of urea and glycerol. However, the oil-water partition coefficient is substantially higher for acetamide than for the other solutes listed in Table II. Similarly, Bean et al. (31) observed that the introduction of ionizable groups, such as acetic acid, into a neutral molecule such as indole drastically reduced the permeability coefficient of the parent solute in similar thin lipid membranes. Thus, for the native membranes, the presence of significant degrees of nonelectrolyte permeability (with reference to water) seemed related, for the most part, to the lipid solubility of the solute in question (for the solutes listed in Table II).

The Effect of Amphotericin B on P_{D_i}

When amphotericin B (10^{-6} M) was present in the aqueous phases bathing the membranes, the results were quite different. It is evident from Table II that the polyene drug produced striking increases in the apparent permeability coefficients of urea, acetamide, glycerol, ribose, and arabinose (in descending order), and that the magnitude of P_{D_i}, in these instances, was inversely related to the effective hydrodynamic radius of the solute tested. As indicated in Table II, clearly detectable counting rates greater than background were obtained in the front (cold) chamber samples from all the flux periods in which these solutes were tested. In contrast, when glucose and sucrose were the aqueous solutes, significant counts in the front chamber samples were present in only 50% and 18%, respectively, of the total number of flux periods (Table II). Since the values of $P_{D_{glucose}}$ and $P_{D_{sucrose}}$ listed in Table II (in the presence of amphotericin B) were computed from the results of the "positive" flux periods, it is likely that they represent maxima. Nevertheless, a comparison of Tables I and II indicates that, under the same experimental conditions (equimolar amounts of cholesterol and phospholipid in the membrane solutions, and 10^{-6} M amphotericin B in the aqueous phases), P_{D_w} was less than twice as great as $P_{D_{urea}}$, approximately 30 times greater than $P_{D_{ribose}}$, and more than 100 times greater than either $P_{D_{glucose}}$ or $P_{D_{sucrose}}$. Consequently, even in the presence of amphotericin B, the relative permeabilities of the latter two solutes were negligible with respect to water (cf. Fig. 6 and Table V).

It is particularly relevant to relate the amphotericin B–dependent increases in the permeability of these membranes to water (Tables I and IV, Fig. 6) and nonelectrolytes (Table II) to the increases in electrical conductance, and, *pari passu*, membrane anion selectivity produced by this drug, or

nystatin, in these thin lipid membranes (4, 5, 8). For this purpose, it was assumed that the changes in nonelectrolyte permeability attributable to amphotericin B were dependent on a common mechanism, and that estimates of $P_{D_{urea}}$ adequately reflected this phenomenon.

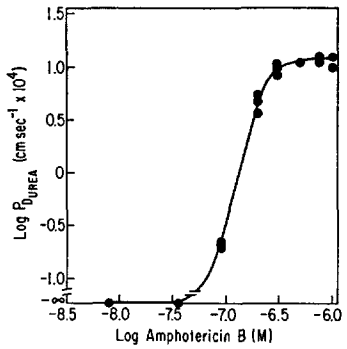

FIGURE 5. The relationship of the log diffusion permeability coefficient of urea ($P_{D_{urea}}$, ordinate) to the log amphotericin B concentration in the aqueous phases bathing the membranes (abscissa). The membrane solution contained equimolar amounts of cholesterol and phospholipid. Experimental details are in Methods.

TABLE III

THE CHOLESTEROL REQUIREMENT OF THE AMPHOTERICIN B–DEPENDENT INCREASE IN $P_{D_{urea}}$

Membrane	Membrane solution: Cholesterol (M) / Phospholipid (M)	Amphotericin B	PD_{urea}
(No.)		(M)	$cm\ sec^{-1} \times 10^4$
3	<0.05	10^{-6}	<0.05 (8)

Thin lipid membranes were formed in the isotope chamber. The aqueous phases bathing the membranes contained 0.01 M urea and 10^{-6} M amphotericin B; ^{14}C-urea (approximately 8×10^6 cpm/ml) was added to the rear chamber. The composition of the membrane solution is indicated in the table, and the value of $P_{D_{urea}}$ was estimated according to Equation 4, from the results of the number of flux periods indicated in parentheses. Experimental details are in Methods.

First, as illustrated in Fig. 5, the increase in $P_{D_{urea}}$ was dependent on a high power of the concentration of amphotericin B in the aqueous phases bathing the membranes. $P_{D_{urea}}$ was unaffected by 10^{-7} M amphotericin B; in the concentration range 10^{-7} M to approximately 3×10^{-7} M amphotericin B, the slope of the relationship between the logarithm $P_{D_{urea}}$ and the logarithm of amphotericin B concentration was approximately 3.5. Similarly, with ref-

erence to Fig. 5, approximately 1.6×10^{-7} amphotericin produces a striking reduction in the DC membrane resistance of these membranes (5). Such a reduction in DC resistance is also proportional to a high power (approximately 4.5 [5]; see also [32]) of the concentration of nystatin, a polyene antibiotic structurally similar to amphotericin B, in the aqueous phases. Second, in agreement with the hypothesis that the primary effects of such polyene antibiotics on these membranes (5, 8; Table I), as on other membrane

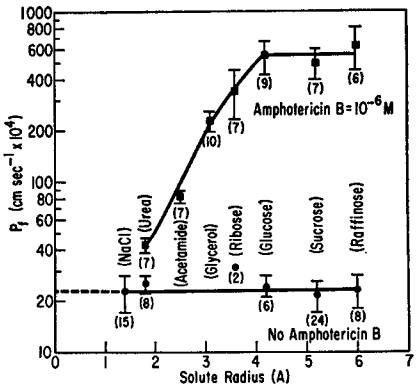

FIGURE 6. The relationship of the osmotic water permeability coefficient (P_f, ordinate) to the effective hydrodynamic radius (abscissa) of the solute in the aqueous phases bathing the membrane. Thin lipid membranes were formed in the osmotic chambers from membrane solutions containing equimolar amounts of cholesterol and phospholipid. The initial aqueous phases contained the indicated solute (0.01 molal) in the presence (squares) or absence (circles) of amphotericin B. For each solute, solutions containing at least two different, higher concentrations of that solute were introduced into the front chamber, so that $\Delta\pi$, the osmotic pressure difference in the two aqueous phases bathing the membranes, was in the range 5 to 16 atm. (Fig. 4). $J_w/\Delta\pi$ was estimated from the slope of plots such as those in Fig. 4, and P_f from Equations 8–10. The values of P_f are indicated as the mean ± SD for the number of observations given, in parentheses. The effective hydrodynamic radius of each of the solutes listed in the figure, except for NaCl and raffinose, is from Schultz and Solomon (27). The effective hydrodynamic radii of NaCl and raffinose are from Pappenheimer et al. (14).

systems (2, 3), are dependent on an interaction with membrane-bound cholesterol, amphotericin B (10^{-6} M) did not produce detectable changes in $P_{D_{urea}}$ when the molar ratio of cholesterol to phospholipid in the membrane solutions was <0.05 (Table III).

Osmotic Flux Experiments

The relevant observations on the osmotic flux experiments (8) are illustrated in Fig. 6 and Tables IV and V. For all the experiments shown in Fig. 6, the lipid solutions used to form membranes contained equimolar amounts of cholesterol and phospholipid. In the absence of amphotericin B, the value of

TABLE IV

AMPHOTERICIN B–DEPENDENT SOLUTE REFLECTION COEFFICIENTS

Solute	P_f	σ_i
	$cm\ sec^{-1} \times 10^4$	
Glucose, sucrose, raffinose	549±143	≈1
Ribose	340±110	0.62±0.25
Glycerol	226±30.8	0.43±0.02
Acetamide	80.8±6.8	0.15±0.04
Urea	42.2±5.4	0.08±0.02

The values of P_f for each of the solutes, in the presence of amphotericin B, were obtained for the indicated solutes from Fig. 6. The P_f values of glucose, sucrose, and raffinose were treated as a single set. The values of σ_i for the remaining solutes were computed from Equation 10, assuming that σ_i was unity for glucose, sucrose, and raffinose, and that L_p was constant. These values are expressed as the mean ± SD (35).

P_f was independent, within experimental error, of the effective hydrodynamic radius of the solute (in the range 1.4 to 6.0 A) in the aqueous phases bathing the membrane (Fig. 6). Thus, under these experimental conditions, σ_i, the reflection coefficient of the ith solute, was probably one for each of the solutes shown in Fig. 6 (8, 11, 18, 19, 32) and P_f, computed from Equation 8 and all the observations in Fig. 6 (in the absence of amphotericin B) was $22.9 \pm 4.6 \times 10^{-4}$ cm sec^{-1} (Table V). This value is in reasonable agreement

TABLE V

THE EFFECTS OF CHOLESTEROL AND AMPHOTERICIN B ON P_f

Membrane solution: Cholesterol (M) / Phospholipid (M)	Aqueous solute	Amphotericin B	P_f
		(M)	$cm\ sec^{-1} \times 10^{-4}$
1	All solutes, Fig. 6	0	22.9±4.6 (64)
1	Glucose, sucrose, raffinose	10^{-6}	549±143 (22)
0.05	Urea	0	33±3.9 (6)
0.05	Urea	10^{-6}	29.2±5.0 (6)
0.05	Raffinose	0	25.5 (3)
0.05	Raffinose	10^{-6}	25.5±2.5 (7)

The values of P_f for membranes formed from lipid solutions containing equimolar amounts of cholesterol and phospholipid are the mean ± SD of all the observations (listed in parentheses) shown in Fig. 6 for the indicated solutes. When the membranes were formed from lipid solutions having a molar ratio of cholesterol to phospholipid <0.05, the aqueous phases contained the indicated solute, and, when listed, amphotericin B. P_f was estimated as described in Methods and Fig. 6, and is expressed as the mean ± SD for the number of observations listed in parentheses.

with the P_f values reported by Price and Thompson (33) and by Everitt et al., (22), and approximately twice as great as the values reported by Finkelstein and Cass for membrane solutions containing equimolar amounts of cholesterol and phospholipid (11, 32, 34).

However, as reported previously (8), when amphotericin B was present in the aqueous phases bathing the membranes, and the membrane solutions contained equimolar amounts of cholesterol and phospholipid, the net flux of water, and consequently the observed value of P_f, varied with the aqueous solute. In the presence of glucose, sucrose, and raffinose, P_f was constant, within the limits of experimental error, and was $549 \pm 143 \times 10^{-4}$ cm sec^{-1} (Fig. 6, Tables IV and V). Although the results are not shown in Fig. 6, P_f had approximately the same value ($607 \pm 85 \times 10^{-4}$ cm sec^{-1}) when NaCl was the aqueous solute, in agreement with the observations of Finkelstein and Cass (32). Assuming that σ_i for glucose, sucrose, and raffinose was unity (cf. Table II), L_p (Equation 10) under these conditions was $4.1 \pm 1.05 \times 10^{-5}$ cm sec^{-1} atm.$^{-1}$ Furthermore, in agreement with the tracer flux measurements (Table II), the net flux of water and the observed value of P_f were reduced (Fig. 6, in the presence of amphotericin B) when solutes whose effective hydrodynamic radii were less than that of glucose were present in the aqueous phases. Table IV lists the values of σ_i which were computed from Equation 10 for the various solutes illustrated in Fig. 6, assuming that L_p was constant. The reported values for σ_i in the presence of nystatin (32) are in reasonable agreement with the data shown in Table IV.

Table V indicates that the value of P_f, like the value of P_{D_w}, was somewhat greater when the amount of cholesterol in the membrane solutions was reduced (34). Under these conditions, the addition of amphotericin B to the aqueous phases did not produce either a reduction in σ_{urea} below one (i.e., P_f was the same when either urea or raffinose was the aqueous solute) or an increase in P_f (Table V). Thus, to the extent that the composition of the membrane solutions reflects the composition of the membranes (5, 8, 31, 34, 36), these data indicate clearly that the amphotericin B–dependent increases in the permeability of these membranes to water (Tables I, IV, and V, Fig. 6) and nonelectrolytes (Tables II and III) were dependent on an interaction with membrane-bound cholesterol.

DISCUSSION

With reference to the dissipative transport of water across membrane systems, two different factors may contribute, singly or in unison, to the production of P_f/P_{D_w} ratios in excess of unity. One such mechanism, suggested originally by Prescott and Zeuthen (37), Koefoed-Johnson and Ussing (38), and Pappenheimer, Renkin, and Borrero (14), and discussed in detail by others (6, 15–17, 21, 24–26, 39–46), depends upon the occurrence of varying degrees

of laminar, or Poiseuille, water flow (i.e., water flow varying with the fourth power of the effective pore radius) through aqueous pores within membranes. The relationship between effective pore radius, laminar water flux, and diffusion water flux is, after Pappenheimer (39) and Robbins and Mauro (21):

$$\beta = \frac{M_p}{M_d} = \frac{r^2RT}{8\eta D_w^o \bar{V}_w} \tag{11}$$

where r = equivalent pore radius, η = coefficient of viscosity, and M_p and M_d are the net fluxes of water due to Poiseuille flow and diffusion flow, respectively. Accordingly,

$$M_t = M_p + M_d \tag{12}$$

where M_t is the total water flux. In these experiments, where σ_i was one,

$$M_t = \frac{L_p}{\bar{V}_w} \times 1 \text{ cm}^2 = \frac{P_f}{RT} \times 1 \text{ cm}^2 \tag{13}$$

where M_t, the total flux of water across a 1 cm² membrane = moles sec^{-1} atm.^{-1} Similarly,

$$M_d = \frac{P_{D_{H_2O}}}{RT} \times 1 \text{ cm}^2, \tag{14}$$

where M_d, the diffusional flux of water across a 1 cm² membrane = moles sec^{-1} atm.^{-1}

In the absence of membrane pores, or when water traverses a membrane solely by diffusion, the presence of unstirred layers in aqueous phases adjacent to the membrane (24–26) may impede isotopic diffusion (when $J_w = 0$) to a substantially greater degree than net water flux (24), and consequently result in P_f/P_{D_w} ratios in excess of one. If such unstirred layers are symmetrical, their total thickness may be related to P_{D_i} by (26):

$$\frac{1}{P_{D_i}} = \frac{1}{P_{t_i}} + \frac{\alpha}{D_i^o} \tag{15}$$

where P_{t_i} = the true permeability coefficient for diffusion of water on the ith solute and α = the sum of the effective thicknesses of the unstirred layers in both aqueous phases adjacent to the membrane.

In the native membranes, despite stirring of the aqueous phases during the THO exchange experiments, the mean ratio P_f/P_{D_w} was slightly in excess of two, when the molar ratio of cholesterol to phospholipid in the membrane solutions was either <0.05 or 1.0 (Tables I, V, and VI). Under similar experimental circumstances (i.e., partition thickness = 1.25×10^{-2} cm,

equimolar amounts of cholesterol and phospholipid in the membrane solutions, and stirring of the aqueous phases in the THO exchange studies), Cass and Finkelstein (11) obtained values of 10.6×10^{-4} cm sec^{-1} and 11.4×10^{-4} cm sec^{-1}, respectively, for P_{D_w} and P_f, and suggested that previously reported values of $P_{D_w} < 5 \times 10^{-4}$ cm sec^{-1} (18, 19) were attributable to unstirred layers in the aqueous phases. Notably, the P_f/P_{D_w} ratio of approximately two observed in the present experiments, in comparison with the studies of Cass and Finkelstein (11), is not attributable to a reduced value for P_{D_w}, but rather to an appreciably higher value for P_f (Fig. 6,

TABLE VI

NATIVE MEMBRANES: THE DIFFERENCE BETWEEN P_{D_w} AND P_f

Membrane solution: Cholesterol (M) / Phospholipid (M)	P_{D_w}	P_f	P_f/P_{D_w}	α	r
	$cm\ sec^{-1} \times 10^4$	$cm\ sec^{-1} \times 10^4$		$cm \times 10^2$	A
1.0	10.8±2.4	22.9±4.6	2.12	1.15	3.8
<0.05	14.0±4.1	31.5±4.2	2.24	0.84	4.0

The values of P_{D_w} are from Table I. The values of P_f are from Table V (all solutes, when the molar ratio of cholesterol to phospholipid in the membrane solutions was one, and for urea and raffinose, when this ratio was <0.05). α, the thickness of the unstirred layers, was computed from Equation 15, assuming $P_{t_w} = P_f$, from the mean values of P_f and P_{D_w}, and using $D^0_w = 2.36 \times 10^{-5}$ cm^2 sec^{-1} (23). The value of r, an equivalent pore radius, was computed from the mean values of P_f and P_{D_w} and Equations 11–14.

Tables V and VI). Similarly, Everitt et al. obtained $P_f = 19 \times 10^{-4}$ cm sec^{-1} and $P_{D_w} = 12.8 \times 10^{-4}$ cm sec^{-1}, when the latter was estimated using both thermal convection and mechanical stirring in the aqueous phases (22). By assuming that $P_f \approx P_{t_w}$ (Equation 15), these workers computed the total thickness of the unstirred layers in their experiments to be approximately 0.07×10^{-2} cm (22). In the present studies, the maximum thickness of the unstirred layer (i.e., if $P_f = P_{t_w}$) was in the range 0.84 to 1.15×10^{-2} cm (Table VI). Alternatively, pores having equivalent radii close to 4.0 A would be required if the difference between P_f and P_{D_w} were solely referable to Poiseuille type flow through aqueous channels (Table VI). However, as estimated both from the net water flux experiments (Fig. 6) and the tracer flux studies (Table II), these thin lipid membranes are considerably less permeable to hydrophilic solutes than would be expected for restricted diffusion through such equivalent pores (6, 14, 15, 42). Thus, it is likely that, in these membranes, the differences between P_f and P_{D_w} are largely attributable to unstirred layers in the aqueous phases adjacent to the membranes (11, 19, 22), and/or experimental error. Stated in another way, these

data are compatible with the hypothesis that the predominant mode of water transfer across such membranes is by a solubility diffusion mechanism (11, 19, 22). Similarly, it is likely that, for the solutes listed in Table II, appreciable degrees of membrane permeation with reference to water (i.e., acetamide), are largely dependent on the lipid solubility of the molecule.

When amphotericin B was added to the aqueous phases, the permeability properties of the membranes were modified to a striking degree. P_{D_w} was increased by approximately 70% (Table I), and the value of P_f was increased 25-fold (Fig. 6, Tables IV and V). Accordingly, the ratio P_f/P_{D_w}, in the presence of amphotericin B, was approximately 30. Concomitantly, the drug increased the permeability of these membranes to certain nonelectrolytes, in inverse relationship to solute size (Tables II and IV, Fig. 6). Furthermore, each of these polyene-dependent effects required the presence of substantial amounts of cholesterol in the membrane solutions (Tables I, III, and V), and, by inference, in the membranes themselves. Accordingly, a reasonable hypothesis is that the interaction of polyene antibiotics, such as amphotericin B (5, 8) or nystatin (5, 32), with membrane-bound cholesterol results in the formation of the equivalent of aqueous channels, or pores, within the membranes.

Since the permeability of the membranes to glucose, and possibly sucrose, was somewhat increased by amphotericin B (Table II), it is likely that the effective pore radius was $\geqq 5.5$ A. However, the possibility of unstirred layers in the aqueous phases adjacent to the membrane, which might have produced erroneously low values of P_{D_w}, precluded the direct application of Equations 11–14 to the calculation of an equivalent pore radius. Rather, estimation of the effective pore radius by the method of Goldstein and Solomon (42) seemed more feasible, since the effects of the unstirred layers on osmotic flow experiments (i.e., Fig. 6) are relatively small with reference to isotope exchange experiments (24). According to Renkin (15), the ratio of the apparent area for filtration of the ith solute (A_{sf}) to that of water (A_{wf}), during bulk flow through aqueous channels, is:

$$\frac{A_{sf}}{A_{wf}} = \frac{\left[2\left(1-\frac{a_i}{r}\right)^2 - \left(1-\frac{a_i}{r}\right)^4\right]\left[1 - 2.104\frac{a_i}{r} + 2.09\left(\frac{a_i}{r}\right)^3 - 0.95\left(\frac{a_i}{r}\right)^5\right]}{\left[2\left(1-\frac{a_w}{r}\right)^2 - \left(1-\frac{a_w}{r}\right)^4\right]\left[1 - 2.104\frac{a_w}{r} + 2.09\left(\frac{a_w}{r}\right)^3 - 0.95\left(\frac{a_w}{r}\right)^5\right]} \quad (16)$$

where r = equivalent pore radius, a_i = effective hydrodynamic radius of the ith solute, and a_w = effective hydrodynamic radius of water (1.5 A [6, 42]). In addition, for solute filtration through aqueous pores (44):

$$\frac{A_{sf}}{A_{wf}} = 1 - \sigma_i - \frac{\omega_i \bar{V}_{s_i}}{L_p} \quad (17)$$

where $\bar{V}_{s_i}$ is the partial molar volume of the ith solute, and only ω_i is deter-

mined when $J_w = 0$. In Fig. 7, the values of A_{sf}/A_{wf}, computed from Equation 17 and the experimental data in Tables II and IV (in the presence of amphotericin B), are plotted in relationship to the theoretical curves computed from Equation 16 and assigned values of 7 A and 10.5 A for the equivalent pore radii. Except for acetamide, which is somewhat anomalous, there is good agreement, within experimental error, between the experimental data and an effective pore radius in the range of 10.5 A.

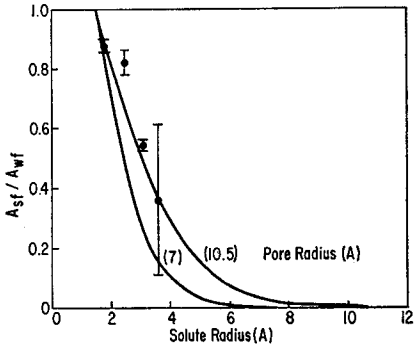

FIGURE 7. A Goldstein-Solomon (42) plot of A_{sf}/A_{wf} (ordinate) as a function of solute radius (abscissa). The two curves were computed from Equation 16, assuming a_w = 1.5 A, for equivalent pore radii of 7 A and 10.5 A. The experimental points were computed from Equation 17, using the mean ω_i values in Table II (in the presence of amphotericin B), the mean ± SD values of σ_i in Table IV, and a mean L_p value of 4.1×10^{-5} cm sec^{-1} atm.$^{-1}$ The latter was computed as indicated in the text (cf. Results).

It should be noted that assigning a value of one for the reflection coefficient of glucose, sucrose, or raffinose (Table IV) represents an approximation, since the range of experimental values in the osmotic flux experiments (Fig. 6) did not permit detection of σ_i values slightly less than one. As indicated by the isotope exchange experiments (Table II), it is likely that σ_{glucose}, and possibly σ_{sucrose}, were somewhat less than one. In this regard, Finkelstein and Cass (32) have reported σ_i values, estimated from osmotic flux studies with nystatin-treated thin lipid membranes, and have suggested that the effective pore radius for such membranes is approximately 4 A. However, the values of A_{sf}/A_{wf}, computed from Equation 17 (neglecting the $\frac{\omega \bar{V}_s}{Lp}$ term) and the σ_i values reported by these authors (32), are in reasonable agreement with the curves (from Equation 16) for pore radii of approximately 12 A, in the case of urea, ethylene glycol, glycerol, and propionamide, or approximately 8 A, in the case or erythritol.

When $J_w = 0$, the equation given by Renkin (15) for restricted diffusion is:

$$\frac{A_{sd}}{A_{wd}} = \frac{\left[1 - \frac{a_i}{r}\right]^2 \left[1 - 2.104\,\frac{a_i}{r} + 2.09\left(\frac{a_i}{r}\right)^3 - 0.95\left(\frac{a_i}{r}\right)^5\right]}{\left[1 - \frac{a_w}{r}\right]^2 \left[1 - 2.104\,\frac{a_w}{r} + 2.09\left(\frac{a_w}{r}\right)^3 - 0.95\left(\frac{a_w}{r}\right)^5\right]} \qquad (18)$$

where A_{sd}/A_{wd} (or, from Equation 7, P'_{D_i}/P'_{D_w}, in a 1 cm² membrane) is the ratio of the apparent area for diffusion of the ith solute to that of water. In Fig. 8, the experimental values of P'_{D_i}/P'_{D_w} (Equation 7; Tables I and II, in the presence of amphotericin B, when the membrane solutions contained equimolar amounts of cholesterol and phospholipid) are plotted in relationship to the theoretical curves computed from Equation 18 for effective pore radii of 7 A and 10.5 A. Within experimental error, the values for the more permeable solutes (urea, acetamide, glycerol, Table II) are in the region of the curve for a pore radius of 10.5 A, while the values for the less

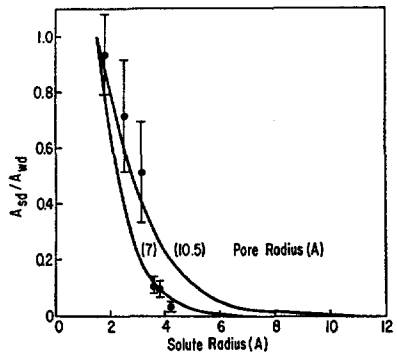

FIGURE 8. The relationship of A_{sd}/A_{wd} (ordinate) to solute radius (abscissa); the curves were drawn from Equation 18, assuming a_w = 1.5 A, for equivalent pore radii of 7 and 10.5 A. The experimental points are the mean ± SD (35) of the ratio P'_{D_i}/P'_{D_w}, computed from the mean ± SD values of P_{D_w} and P_{D_i} in, respectively, Tables I and II (when the aqueous phases contained amphotericin B, and the membrane solutions contained equimolar amounts of cholesterol and phospholipid), and Equation 7.

permeable solutes (ribose, arabinose, glucose, Table II) are in good agreement with the curve for a pore radius of 7 A. The reasons for the apparently bimodal distribution of the experimental values are not clear. In addition to experimental error, the phenomenon might relate to a heterogeneous population of pores with varying radii. Alternatively, the factors considered in Equation 18 which restrict diffusion include steric hindrance at the entrance to the pore (14, 15) and the frictional effect of the diffusing molecules within the pore (15). Consequently, if there are additional restrictions to the diffusion of water and/or solute through narrow pores in these membranes, Equation 18 might not be directly applicable. Lastly, the presence of unstirred layers in the aqueous phases adjacent to the membranes might have reduced the actual value of P_{D_w}, and, to a lesser extent, of P'_{D_i} for the more permeable solutes (i.e., urea, acetamide, or glycerol). However, taken together, the data in Figs. 7 and 8 suggest that, to a rational approximation, the equivalent radius of the amphotericin B–dependent pores within these membranes is in the range 7 to 10.5 A.

Assuming these values for the pore radii, certain additional inferences are possible. Poiseuille's equation for laminar flow in aqueous channels is:

$$\frac{A_o}{\Delta x} = \frac{M_p 8\eta \bar{V}_w}{r^2} \tag{19}$$

where r^2 = pore radius and $A_o/\Delta x$ = actual pore area per unit membrane thickness (centimeters) for a 1 cm² membrane. When σ_i is one, substituting from Equations 11–13, we have:

$$\frac{A_o}{\Delta x} = \left(\frac{\beta}{\beta + 1}\right)\frac{P_f 8\eta \bar{V}_w}{RTr^2}. \tag{20}$$

TABLE VII

PROPERTIES OF AMPHOTERICIN B-TREATED THIN LIPID MEMBRANES

r_p	$A_0/\Delta x$	P'_{t_w}	P'_{D_w}	α
A	*cm*	*cm*	*cm*$^{-1}$	*cm* × 10²
7	485	171	76.8	0.72
10.5	242	126	76.8	0.50

$A_0/\Delta x$ was computed from Equation 20, using P_f = 549 × 10^{-4} cm sec^{-1} (Table V) for pore radii of 7 and 10.5 A. The corresponding values of P'_{t_w} were computed from Equation 21. The values of P'_{D_w} were obtained using P_{D_w} = 18.1 × 10^{-4} cm sec^{-1} (Table I) and Equation 7; the values of α, the thickness of the unstirred layer, were computed from the indicated values of P'_{t_w}, P'_{D_w}, and Equation 15.

Furthermore, for restricted diffusion through aqueous pores, the effective area per unit membrane thickness (P'_{t_w}, for a 1 cm² membrane) for water diffusion is, according to Renkin (15):

$$P'_{t_w} = \frac{A_o}{\Delta x}\left(1 - \frac{a_w}{r}\right)^2\left[1 - 2.104\left(\frac{a_w}{r}\right) + 2.09\left(\frac{a_w}{r}\right)^3 - 0.95\left(\frac{a_w}{r}\right)^5\right] \tag{21}$$

Table VII lists the values of $A_o/\Delta x$ (Equation 20) and P'_{t_w} (Equation 21) computed for pore radii of 7 and 10.5 A, using P_f = 549 × 10^{-4} cm sec^{-1} (Table V); i.e., the value for membranes formed from lipid solutions containing equimolar amounts of cholesterol and phospholipid, when amphotericin B was present in the aqueous phases. It is reasonable to suppose that the differences between P'_{t_w} and the corresponding values of P'_{D_w} (Tables I and VII) are attributable to unstirred layers in the aqueous phases. Applying these values to Equation 15, the thickness of the unstirred layers is in the range 0.5 to 0.72 × 10^{-2} cm (Table VII), in reasonable agreement with the value of Everitt et al. (22), and less than the maximal values calculated for α in

Table VI. Lastly, assuming a membrane thickness of 60 A (12), the fractional pore areas (from $A_o/\Delta x$) would be 1.03×10^{-4} or 0.76×10^{-4}, respectively, for pore radii of 7 A or 10.5 A.

The nature of the interactions between amphotericin B and membrane-bound cholesterol which may result in the formation of aqueous pores in these membranes is not known, nor is it understood whether such interactions are directly or cooperatively (i.e., by interaction with membrane-bound phospholipids) responsible for the changes in membrane permeability. In monomolecular lipid layers, Demel et al. (47) have provided evidence that the 3-OH group of cholesterol may have a primary role in the interaction with polyene drugs. Hopefully, structure-function studies with different sterols and polyene antibiotics, currently in progress in our laboratory, may provide some information concerning the molecular requirements for sterol-polyene interactions which result in pore formation in these membranes.

The authors are grateful to Drs. D. C. Tosteson and Paul Horowicz for the benefit of many valuable discussions, and to Dr. D. C. Tosteson for his support of the project.

We are grateful to Mrs. Elizabeth Herndon for her able technical assistance.

This work was supported by a grant from the National Science Foundation (GB 6714) and by a grant from the American Heart Association (68659), supported in part by the North Carolina Heart Association. One of the authors (T. E. A.) was supported by a Public Health Service Career Development Award (PHS 1-K3-GM-18, 161) from the National Institute of General Medical Sciences. Dr. Dennis was supported by a Postdoctoral Fellowship (1-F2-GM-35,738) from the National Institutes of Health.

Received for publication 27 August 1968.

REFERENCES

1. Oroshnik, W., and A. D. Mebane. 1963. The polyene antifungal antibiotics. *Fortschr. Chem. Org. Naturst.* 17.
2. Kinsky, S. C., S. A. Luse, and L. L. M. Van Deenen. 1966. Interaction of polyene antibiotics with natural and artificial membrane systems. *Fed. Proc.* **25**:1503.
3. Lampen, J. O. 1966. Interference by polyene antifungal antibiotics (especially nystatin and filipin) with specific membrane functions. *Symp. Soc. Gen. Microbiol.* **16**:111.
4. Andreoli, T. E., and M. Monahan. 1968. Polyene-dependent anion selectivity in thin lipid membranes. Abstracts of the Biophysical Society 12th Annual Meeting. Pittsburgh, Pa. A-23.
5. Andreoli, T. E., and M. Monahan. 1968. The interaction of polyene antibiotics with thin lipid membranes. *J. Gen. Physiol.* **52**:300.
6. Solomon, A. K. 1968. Characterization of biological membranes by equivalent pores. *J. Gen. Physiol.* **51**:335s.
7. Spiegler, K. S. 1958. Transport processes in ionic membranes. *Trans. Faraday Soc.* **54**:1409.
8. Andreoli, T. E., V. W. Dennis, and M. Monahan. 1968. The effects of polyene antibiotics on electrical and osmotic properties of thin lipid membranes. *J. Clin. Invest.* **47**:1a.
9. Andreoli, T. E., J. A. Bangham, and D. C. Tosteson. 1967. The formation and properties of thin lipid membranes from HK and LK sheep red cell lipids. *J. Gen. Physiol.* **50**:1729.
10. Mueller, P., D. O. Rudin, H. Titien, and W. C. Wescott. 1962. Reconstitution of excitable cell membrane structure in vitro. *Circulation.* **26**:1167.

11. CASS, A., and A. FINKELSTEIN. 1967. Water permeability of thin lipid membranes. *J. Gen. Physiol.* **50**:1765.
12. HUANG, C., L. WHEELDON, and T. E. THOMPSON. 1964. The properties of lipid bilayer membranes separating two aqueous phases: formation of a membrane of simple composition. *J. Mol. Biol.* **8**:148.
13. BRAY, G. E. 1960. A simple efficient liquid scintillator for counting aqueous solutions in a liquid scintillation system. *Anal. Biochem.* **1**:279.
14. PAPPENHEIMER, J. R., E. M. RENKIN, and L. M. BORRERO. 1951. Filtration, diffusion, and molecular seiving through peripheral capillary membranes. *Amer. J. Physiol.* **167**:13.
15. RENKIN, E. M. 1955. Filtration, diffusion and molecular seiving through porous cellophane membranes. *J. Gen. Physiol.* **38**:225.
16. KEDEM, O., and A. KATCHALSKY. 1958. Thermodynamic analysis of the permeability of biological membranes to non-electrolytes. *Biochim. Biophys. Acta.* **27**:229.
17. KEDEM, O., AND A. KATCHALSKY. 1961. A physical interpretation of the phenomenological coefficients of membrane permeability. *J. Gen. Physiol.* **45**:143.
18. HUANG, C., and T. E. THOMPSON. 1966. Properties of lipid membranes separating two aqueous phases: water permeability. *J. Mol. Biol.* **15**:539.
19. HANAI, T., and D. A. HAYDON. 1966. The permeability to water of bimolecular lipid membranes. *J. Theor. Biol.* **11**:370.
20. STAVERMAN, H. J. 1951. The theory of measurement of osmotic pressure. *Rec. Trav. Chim. Pays-Bas.* **70**:344.
21. ROBBINS, E., and A. MAURO. 1960. Experimental study of the independence of diffusion and hydrodynamic permeability coefficients in collodion membranes. *J. Gen. Physiol.* **43**:523.
22. EVERITT, C. T., W. R. REDWOOD, and D. A. HAYDON. 1968. The problem of boundary layers in the exchange diffusion of water across bimolecular lipid membranes. *J. Theor. Biol.* In press.
23. WANG, J. H., C. V. ROBINSON, and I. S. EDELMAN. 1953. Self-diffusion and structure of water. III. Measurement of the self-diffusion of liquid water with H^2, H^3 and O^{18} as tracers. *J. Amer. Chem. Soc.* **75**:466.
24. DAINTY, J. 1963. Water relations of plant cells. *Advan. Bot. Res.* **1**:279.
25. GINZBURG, B. Z., and A. KATCHALSKY. 1963. The frictional coefficients of the flows of non-electrolytes through artificial membranes. *J. Gen. Physiol.* **47**:403.
26. DAINTY, J., and C. R. HOUSE. 1966. "Unstirred layers" in frog skin. *J. Physiol. (London).* **182**:66.
27. SCHULTZ, S. G., and A. K. SOLOMON. 1961. Determination of effective hydrodynamic radii of small molecules by viscometry. *J. Gen. Physiol.* **44**:1189.
28. SOLL, A. H. 1967. A new approach to molecular configuration applied to aqueous pore transport. *J. Gen. Physiol.* **50**:2565.
29. COLLANDER, R., and H. BARLUND. 1933. Permeabilitatsstudien an Characeratophylla. II. Die permeabilitat fur nichtelectrolyte. *Acta Bot. Fenn.* **11**:5.
30. VREEMAN, H. J. 1966. Permeability of thin phospholipid films. *Kon. Ned. Akad. Wetensch. Proc. Ser. B. Phys. Sci.* **69**:542.
31. BEAN, R. C., H. CHEN, C. J. D'AGOSTINO, JR., J. T. EICHNER, H. A. ELLS, R. E. KAY, H. A. PARKER JONES, W. C. SHEPHERD, and L. SMITH, JR. 1967. Transport of macromolecules across biological membranes. Philco-Ford Rept. No. V-4184. Philco-Ford Corp., Newport Beach, R.I. 72.
32. FINKELSTEIN, A., and A. CASS. 1968. Permeability and electrical properties of thin lipid membranes. *J. Gen. Physiol.* **52**:145s.
33. PRICE, H. D., and T. E. THOMPSON. 1968. Lipid bilayer membranes: temperature dependence of osmotic water permeability. Abstracts of the Biophysical Society 12th Annual Meeting. Pittsburgh, Pa. A-24.
34. FINKELSTEIN, A., and A. CASS. 1967. Effect of cholesterol on the water permeability of thin lipid membranes. *Nature.* **216**:717.

35. OVERMAN, R. T., and H. M. CLARK. 1960. Radioisotope techniques. McGraw-Hill Book Co., New York. 109.
36. HANAI, T., D. A. HAYDON, and J. TAYLOR. 1965. The influence of lipid composition and of some adsorbed proteins on the capacitance of black hydrocarbon membranes. *J. Theor. Biol.* **9**:422.
37. PRESCOTT, D. M., and E. ZEUTHEN. 1952. Comparison of water diffusion and water filtration across cell surfaces. *Acta Physiol. Scand.* **28**:77.
38. KOEFOED-JOHNSON, V., and H. H. USSING. 1953. The contributions of diffusion and flow to the passage of D_2O through living membranes. *Acta Physiol. Scand.* **28**:60.
39. PAPPENHEIMER, J. R. 1953. Passage of molecules through capillary walls. *Physiol. Rev.* **33**: 387.
40. DURBIN, R. P., H. FRANK, and A. K. SOLOMON. 1956. Water flow through gastric mucosa. *J. Gen. Physiol.* **39**:535.
41. PAGANELLI, C. V., and A. K. SOLOMON. 1957. The rate of exchange of tritiated water across the human red cell membrane. *J. Gen. Physiol.* **41**:259.
42. GOLDSTEIN, D. A., and A. K. SOLOMON. 1960. Determination of equivalent pore radius for human red cells by osmotic pressure measurement. *J. Gen. Physiol.* **44**:1.
43. DURBIN, R. P. 1960. Osmotic flow of water across permeable cellulose membranes. *J. Gen. Physiol.* **44**:315.
44. DAINTY, J. R., and B. Z. GINZBURG. 1963. Irreversible thermodynamics and frictional models of membrane processes, with particular reference to the cell membrane. *J. Theor. Biol.* **5**:256.
45. LONGUET HIGGINS, H. C., and G. AUSTIN. 1966. The kinetics of osmotic transport through pores of molecular dimensions. *Biophys. J.* **6**:217.
46. MICKULECKY, D. C. 1967. On the relative contributions of viscous flow vs. diffusional (frictional) flow to the stationary state flow of water through a "tight" membrane. *Biophys. J.* **7**:527.
47. DEMEL, R. A., F. J. L. CROMBAG, L. L. M. VAN DEENEN, and S. C. KINSKY. 1968. Interaction of polyene antibiotics with single and mixed lipid monomolecular layers. *Biochim. Biophys. Acta.* **150**:1.